Hindawi Publishing Corporation
Journal of Sensors
Volume 2010, Article ID 452163, 7 pages
doi:10.1155/2010/452163

Research Article

Real-Time Noninvasive Measurement of Glucose Concentration Using a Microwave Biosensor

Arsen Bababjanyan,[1] Harutyun Melikyan,[1] Seungwan Kim,[1] Jongchel Kim,[1] Kiejin Lee,[1] and Barry Friedman[2]

[1] *Department of Physics and Basic Science Institute for Cell Damage Control, Sogang University, Seoul 121-742, Republic of Korea*
[2] *Department of Physics, Sam Houston State University, Huntsville, TX 77341, USA*

Correspondence should be addressed to Kiejin Lee, klee@sogang.ac.kr

Received 27 February 2010; Accepted 13 December 2010

Academic Editor: Hai Xiao

We measured the glucose concentration by using the real-time electromagnetic interaction between probe-tip and glucose solution using a microwave biosensor. The microwave biosensor, consisting of a dielectric resonator coupled to the probe-tip, allows observation of the small variation of the glucose concentration changes in the ranges of 0–300 mg/ml by measuring the microwave reflection coefficient S_{11}. We could observe the concentration of glucose with a detectable resolution up to 1 mg/ml at an operating frequency of about $f = 4\text{-}5$ GHz. The change of the glucose concentration is directly related to the change of the reflection coefficient due to the electromagnetic interaction between the microwave resonator and the glucose solution. The operational principal is explained by the plane-wave solution model. The measured signal-to-noise ratio was about 37 dB, and the minimum detectible signal was about 0.003 dB/(mg/ml). A glucose biosensor using a microwave resonator with probe provides a unique approach for glucose real-time monitoring.

1. Introduction

The real-time detection and the quantification of glucose concentration with high sensitivity, selectivity, and accuracy are required in many different areas. Accurate and rapid measurement of the glucose concentration is very important in biological analysis and clinical monitoring and in the food processing industry [1, 2]. The food, beverage, and pulp industries require simple, fast, and economic analytical methods in order to control fermentation and for quality-control processes. Accurate measurements of the dielectric properties of glucose in aqueous solutions are essential for both fundamental studies and biomedical applications.

Glucose biosensors have taken several forms, based on electrochemical, optical, piezoelectrical, thermal, and mechanical principles [3–9]. Most of sensors are based on electrochemical principles and employ enzymes for molecular recognition. Though the first amperometric enzymatic glucose biosensor was developed in the 1960s, the amperometric enzymatic principle is still of interest to many researchers because of its high selectivity to glucose [5, 7]. Devices incorporating this technology have already passed the stage of proof of concept. Amperometric enzyme electrodes hold a leading position among present glucose biosensor systems and have already found a large commercial market. Recently, a number of mechanically based glucose biosensors based on the cantilever platform have been demonstrated and found to respond specifically to the correct analyte over a wide concentration range [4, 6]. Optical glucose biosensors are exploiting electromagnetic wave interactions with the glucose solution on the sensor surface to allow real-time analytical-evaluation of glucose [8, 9]. Commercial development of these devices has allowed measurement of glucose concentration with sufficient accuracy for several applications. However, the existing devices are largely limited to monitoring patterns and trends or are invasive. Efforts are now being made to find new technology noninvasive, quantitative real-time glucose monitoring. Techniques with high sensitivity and efficiency for the detection of glucose concentration using a noninvasive technology

are therefore of importance in biosensor construction. In order to better characterize the concentration of glucose, we take advantage of the noninvasive evaluation capabilities of a real-time interaction technique using a microwave biosensor [10–14]. The microwave waveguide resonator biosensor is a new physical approach to real-time determination of the glucose concentration.

In this paper, we monitored the glucose concentration by using a microwave sensing technique in real-time [15–19]. The changes in the glucose concentration due to a change in the permittivity of the glucose solution were investigated by measuring the microwave reflection coefficient S_{11} of probe/sample system. The change in the glucose concentration was directly related to the change in the intensity of the reflection coefficient S_{11} due to an electromagnetic interaction between the microwave probe-tip and the glucose solution.

2. Experimental

2.1. Apparatus. We fabricated the biosensor based on the microwave resonator. The experimental setup of the microwave biosensor is shown in Figure 1(a). The microwave biosensor consisted of a high Q-factor dielectric resonator coupled to an Au probe-tip [20]. The resonance frequency of a given TE_{011} mode was about 4.6 GHz. The $Ba(ZrTa)O_3$ dielectric cylindrical resonator with dielectric constant $\varepsilon = 29$ has inner and outer diameters of 2 mm and 14 mm, respectively, and a height of 5.8 mm. The diameter of the metal cylindrical cavity is 32 mm, and the height is 14 mm. The dielectric resonator has a fixed resonance frequency determined by the material, dimensions, and the shielding cavity parameters. In order to achieve the best possible sensitivity, we tuned the resonance frequency and the impedance simultaneously by adjusting the tuning screw before scanning over the sample. To obtain high sensitivity of the biosensor, a gold coated probe-tip with a round apex (and with a diameter of 1 mm) and cylindrical end was used and attached to the inner loop of the resonator.

The silicon tube with wall thickness $t_t = 0.4$ mm and inner diameter $t_g = 2.5$ mm was mounted on the cylindrical end of the probe-tip as shown in Figure 1(b). The entire system was placed on a mechanical vibration isolation table, and measurements were performed inside an electromagnetically shielded environment with automated temperature and humidity control. The glucose flows inside the tube with the constant $v_g = 2$ mm/s speed. To determine the glucose concentration changes, we measured the reflection coefficient S_{11} of the microwave resonator using a network analyzer. At the start of measurement the input loop and resonator impedances are matched, by adjustment of the tuning screw and positioning of the dielectric resonator, to minimize the reflection coefficient S_{11}. Subsequent changes in electromagnetic coupling between the probe-tip and the sample cause an increase in the magnitude of S_{11}, and this forms the basis of sample characterization. All measurements were done at 37°C. At resonance, for the given mode TE_{011}, the unloaded Q-factor was 24,000, and the probe-tip characteristic impedance was $Z_0 = 50\,\Omega$.

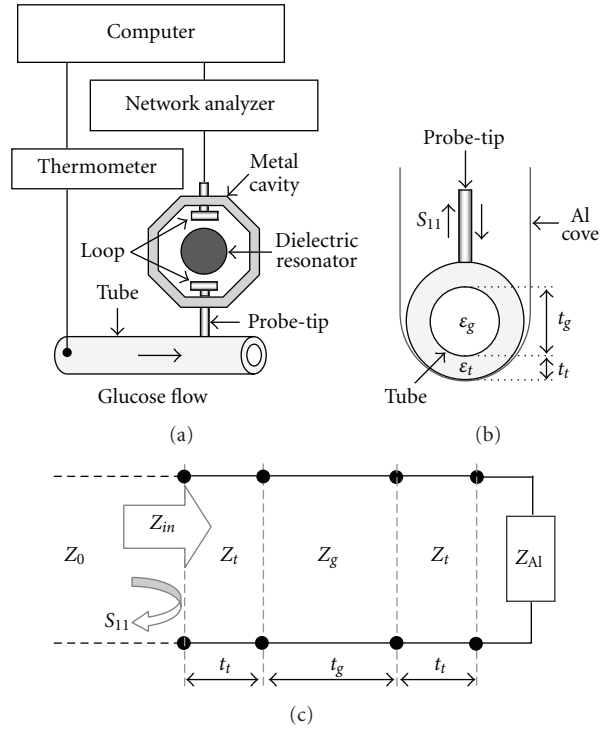

Figure 1: (a) Experimental setup, (b) tip-sample configuration, and (c) equivalent impedance model of microwave biosensor.

2.2. Plane-Wave Solution. The microwave reflection principle can be explained by the plane-wave solution model. Figure 1(c) presents the equivalent impedance model of the probe-sample configuration. An interpretation of the reflection coefficient S_{11} magnitude in terms of medium parameters is written as [21]

$$S_{11} = 20\log\left|\frac{|Z_{\text{in}}| - Z_0}{|Z_{\text{in}}| + Z_0}\right|, \tag{1}$$

where S_{11} is the reflection coefficient, Z_0 is the characteristic impedance of the probe tip, and Z_{in} is the complex input impedance of the tube/glucose/tube/Al system, and it can be estimated as

$$\begin{aligned} Z_{\text{in}} &= Z_t\frac{Z_{gt\text{Al}} + jZ_t\tan(k_t t_t)}{Z_t + jZ_{gt\text{Al}}\tan(k_t t_t)} \\ &\cong jZ_a k_a\frac{\left(2t_g + t_t\right) - k_a^2 t_t t_g^2\varepsilon_g}{1 - k_a^2 t_g\varepsilon_t\left(t_g + t_t\right) - k_a^2 t_t t_g\varepsilon_g}, \end{aligned} \tag{2}$$

where Z_t and Z_a ($Z_a = 377\,\Omega$) are the complex impedance of the silicon tube and air, k_t and k_a ($k_a = 96\,\text{m}^{-1}$ at 4.6 GHz) are the wave vector in the silicon tube and in air, t_t and t_g are the wall thickness and diameter of the cylindrical silicon tube, respectively. ε_g is the dielectric permittivity of the glucose solution, and $Z_{gt\text{Al}}$ is the complex impedance of

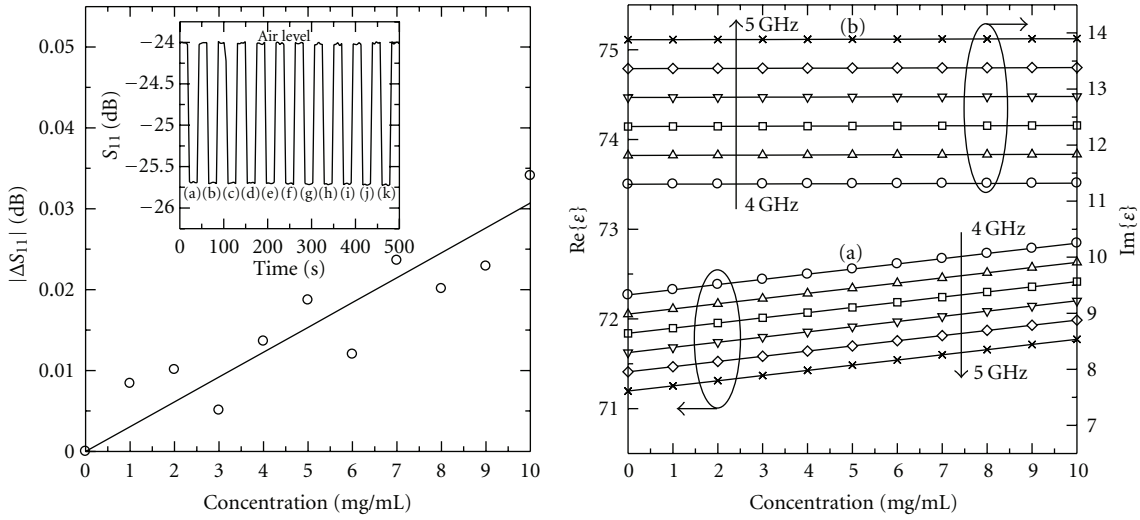

FIGURE 2: (a) Measured microwave reflection coefficient change ΔS_{11} plotted as a function of the glucose concentrations from DI water to 10 mg/ml with the interval of 1 mg/ml at 4.6 GHz (low concentration range). A solid line shows a fit to (1) and (4) with $Z_0 = 50\,\Omega$. The inset shows the real-time diagram of the microwave reflection coefficient with two signal levels: for air, that is, empty tube and for (a) DI water or glucose solution with the glucose concentration of (b) 1 mg/ml, (c) 2 mg/ml, (d) 3 mg/ml, (e) 4 mg/ml, (f) 5 mg/ml, (g) 6 mg/ml, (h) 7 mg/ml, (i) 8 mg/ml, (j) 9 mg/ml, and (k) 10 mg/ml. (b) The dependences of (a) real (left axis) and (b) imaginary (right axis) parts of the complex relative permittivity on the glucose concentration (low concentration range: 0–10 mg/ml) as a function of operation frequency in the 4-5 GHz range.

the glucose/tube/Al system and is given by the expression

$$Z_{gt\mathrm{Al}} = Z_g \frac{Z_{t\mathrm{Al}} + jZ_g \tan\left(k_g t_g\right)}{Z_g + jZ_{t\mathrm{Al}} \tan\left(k_g t_g\right)} \cong \frac{jZ_a k_a \left(t_t + t_g\right)}{1 - k_a^2 t_t t_g \varepsilon_g}, \tag{3}$$

where Z_g and k_g are the complex impedance and wave vector of glucose solution, respectively, and $Z_{t\mathrm{Al}}$ is the complex impedance of the silicon tube/Al system (this is similar to a dielectric on perfect metal system [22]), and it can be expressed as

$$\begin{aligned} Z_{t\mathrm{Al}} &= jZ_t k_t t_t = j \cdot Z_a \sqrt{\frac{\mu_t}{\varepsilon_t}} \cdot k_a \sqrt{\mu_t \varepsilon_t} \cdot t_t \\ &= jZ_a k_a \mu_t t_t \cong jZ_a k_a t_t. \end{aligned} \tag{4}$$

Here ε_t and μ_t are the relative dielectric permittivity and the relative magnetic permeability ($\mu_t \approx 1$) of the silicon tube.

The dependence of permittivity on glucose concentration is approximately linear and is often expressed by the molar increment, δ: $\varepsilon_g = \varepsilon_w + c\delta$, where ε_w is the relative permittivity of water ($\varepsilon_w = 71.62$ at 4.6 GHz, for 37°C [23]), c is the concentration of the glucose in mg/ml, and δ is the increase in permittivity when the glucose concentration is raised by 1 unit ($\delta = 0.0577\,(\mathrm{mg/ml})^{-1}$ [17]).

3. Results and Discussion

3.1. Low Concentration Range. Figure 2(a) shows the microwave reflection coefficient change ΔS_{11} dependence of glucose concentration ranging from deionized (DI) water (i.e., no glucose) to 10 mg/ml glucose concentration with an interval of 1 mg/ml. Clear changes in the microwave resonance were observed as the glucose concentrations were increased. The intensity of S_{11} for the tube without (i.e., with air which is the reference level of S_{11} for our measurements) and with DI water was −24 dB and −25.69 dB, respectively. During the real-time measurement firstly the silicon tube is filled by DI water, and then it is continuously filled by glucose solution with the different concentrations. The maximum intensity of the reflection coefficient is observed for the sample with the concentration 10 mg/ml with a monotonic decrease between the minimum and maximum concentrations of the solution. Clearly the change in the relative permittivity of the glucose solution affected the change in the microwave reflection ΔS_{11}. As the concentration increased, the dielectric permittivity of the glucose solution increased, and the intensity of the reflection coefficient S_{11} almost linearly increased (in absolute value) as expected from (1) and as shown in the Figure 2(a). The inset demonstrates the real-time diagram of the microwave reflection coefficient for (a) DI water and for glucose with concentration of (b) 1 mg/ml, (c) 2 mg/ml, (d) 3 mg/ml, (e) 4 mg/ml, (f) 5 mg/ml, (g) 6 mg/ml, (h) 7 mg/ml, (i) 8 mg/ml, (j) 9 mg/ml, and (k) 10 mg/ml. The relative permittivity of the glucose solution may be estimated by the intensity of the reflection coefficient at the resonance frequency. We found a good agreement with theory between the variation of reflection coefficient S_{11} and the glucose concentrations. Figure 2(b) shows the estimated (a) real and (b) imaginary parts of the complex relative dielectric permittivity of the glucose solution at the 4-5 GHz range

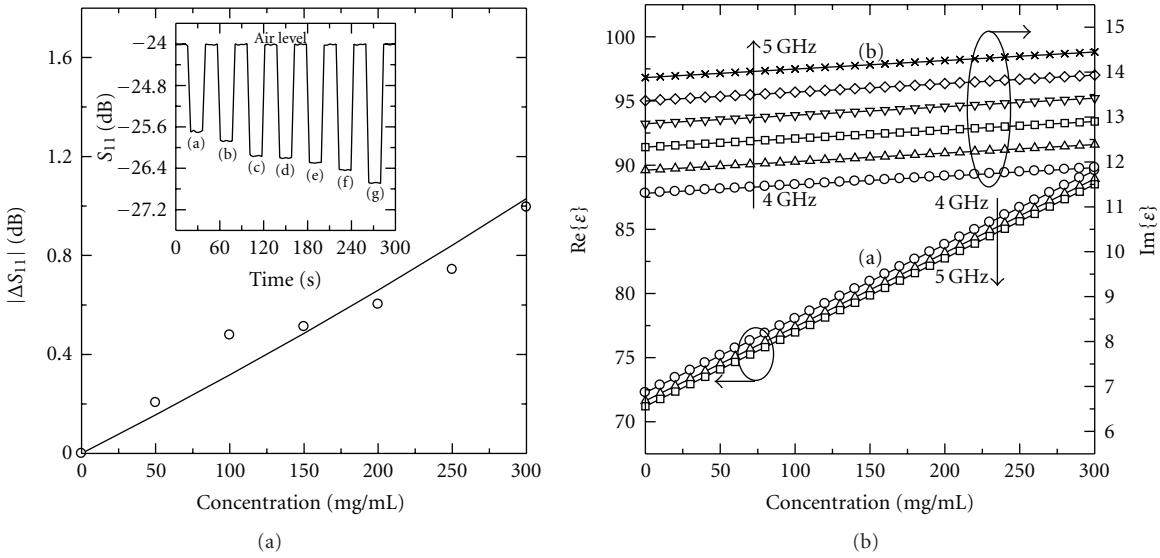

(a) (b)

Figure 3: (a) Measured microwave reflection coefficient change ΔS_{11} plotted as a function of the glucose concentrations from DI water to 300 mg/ml with the interval of 50 mg/ml at 4.6 GHz (high concentration range). The inset (a) shows real-time diagram of the microwave reflection coefficient with two signal levels: for air, that is, empty tube and for (a) DI water or glucose solution with the glucose concentration of (b) 50 mg/ml, (c) 100 mg/ml, (d) 150 mg/ml, (e) 200 mg/ml, (f) 250 mg/ml, and (g) 300 mg/ml. (b) The dependences of (a) real (left axis) and (b) imaginary (right axis) parts of the complex relative permittivity on the glucose concentration (0–300 mg/ml) as a function of operation frequency in the 4-5 GHz range.

plotted as a function of the glucose concentration in the low concentration range (up to 10 mg/ml). The temperature of the glucose solution was 37 ± 0.1°C. Both real and imaginary parts of the complex relative permittivity show the same increasing behavior (incidentally, the real part increased more quickly than imaginary part; $\Delta\varepsilon' = 1.08$ versus $\Delta\varepsilon'' = 0.02$ at 4.4 GHz over the range of glucose concentration up to 10 mg/ml) with increase of glucose concentration. However, the frequency dependences of the real and imaginary permittivity were different. If real part of the relative permittivity decreased (from 72.84 to 71.77 for 10 mg/ml), the imaginary part of the relative permittivity increased (from 11.32 to 13.89 for 10 mg/ml) with the increase of operation frequency from 4 GHz to 5 GHz.

3.2. High Concentration Range. Figure 3(a) shows the microwave reflection coefficient change ΔS_{11} dependence of glucose concentrations ranging from DI to 300 mg/ml glucose concentration with an interval of 50 mg/ml. Again, the clear changes in the microwave resonance were observed as the glucose concentrations were increased. The change in concentration of glucose affected the change in the relative permittivity of the solution. As the concentration increased, the dielectric permittivity of the glucose solution increased, and the intensity of the reflection coefficient S_{11} almost linearly increased (in absolute value). The inset demonstrates the real-time diagram of the microwave reflection coefficient for (a) DI water and for glucose solution with glucose concentration of (b) 50 mg/ml, (c) 100 mg/ml, (d) 150 mg/ml, (e) 200 mg/ml, (f) 250 mg/ml, and (g) 300 mg/ml. Figure 3(b) shows the estimated (a) real and (b) imaginary parts of the complex relative dielectric permittivity of the glucose solution in the 4-5 GHz range plotted as a function of the glucose concentration in the high concentration range (up to 300 mg/ml). The temperature of the glucose solution was 37 ± 0.1°C. The real part of the relative permittivity decreased (from 89.58 to 88.51 for 300 mg/ml), and the imaginary part of the relative permittivity increased (from 11.87 to 13.93 for 300 mg/ml) with an increase of operation frequency from 4 GHz to 5 GHz.

The relationship of microwave reflection coefficient S_{11} as a function of glucose concentration at lower glucose concentrations is $\Delta S_{11}/\Delta c = 0.0031$ dB/(mg/ml) or $2 \cdot 10^{-5}$ (mg/ml)$^{-1}$ in the linear range. The root-mean-square statistical noise in S_{11} for our system is about 10^{-7} [17, 18]. The measured signal-to-noise ratio (SNR) was about 37 dB. The smallest detectable change in concentration based on a criterion of SNR of 37 dB was about 1 mg/ml. By increasing the Q-factor of the resonator, the slope becomes steeper, and the sensitivity can be further enhanced.

3.3. Temperature Effect. Due to the sensitivity of the relative permittivity of the glucose solution to temperature, the reflection coefficient S_{11} is strongly dependent on temperature of the solution. Figure 4(a) shows the reflection coefficient S_{11} dependence on the temperature for the (a) DI water and for the glucose solution with the glucose concentration of (b) 10 mg/ml, (c) 100 mg/ml, and (d) 200 mg/ml. When the temperature of the glucose solution increased from 32°C to 42°C, the reflection coefficient S_{11} increased due to the decrease of the relative permittivity of

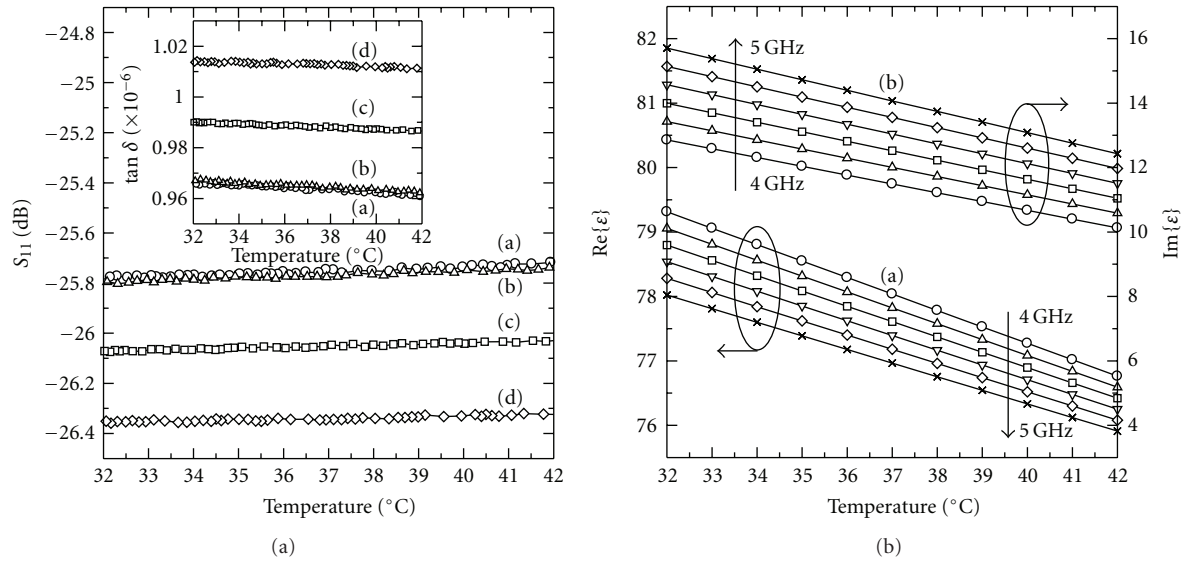

FIGURE 4: (a) Measured microwave reflection coefficient S_{11} plotted as a function of the temperature of the glucose solution in the range 32–42°C at 4.6 GHz for (a) DI water and glucose solution with concentration of (b) 10 mg/ml, (c) 100 mg/ml, and (d) 200 mg/ml. The inset shows the measured loss tangent tan δ plotted as a function of the temperature for the DI water and the same concentrations of glucose. (b) The dependences of (a) real (left axis) and (b) imaginary (right axis) parts of the relative permittivity on the glucose solution temperature (32–42°C) as a function of operation frequency in the 4-5 GHz range. The glucose concentration was 100 mg/ml.

glucose solution as shown in Figure 4(b). We observed that the temperature coefficient variation of reflection coefficient ΔS_{11} for 10 mg/ml, 100 mg/ml, and 200 mg/ml glucose solution was about 0.022%/°C, 0.017%/°C, and 0.012%/°C, respectively. As the concentration of the glucose solutions increased, temperature coefficient variations are decreased. Note that the variation in the real part of the complex relative permittivity was on the order 0.32%/°C, 0.29%/°C, and 0.27%/°C for 10 mg/ml, 100 mg/ml, and 200 mg/ml glucose solution, respectively. The inset of Figure 4(a) shows the value of loss tangent ($\tan\delta = \varepsilon''/\varepsilon'$) of solution at microwaves as a function of temperature for the (a) DI water and for the glucose concentration of (b) 10 mg/ml, (c) 100 mg/ml, and (d) 200 mg/ml. The tan δ of glucose solution decreased as the temperature increased due to the real and imaginary part of the complex relative permittivity of glucose decreasing (see Figure 4(b)). Note that, as the temperature of the glucose solution increased, the imaginary part of the complex relative permittivity of glucose ε'' decreases more rapidly than that of real part ε' ($\Delta\varepsilon'' = 2.95$ versus $\Delta\varepsilon' = 2.37$ at 4.4 GHz for the glucose concentration of 100 mg/ml), hence tan δ decreased. Figure 4(b) shows the estimated (a) real and (b) imaginary parts of the complex relative dielectric permittivity of the 100 mg/ml glucose solution plotted as a function of the temperature of the glucose solution in the 4-5 GHz range. The real part of the complex relative permittivity decreased (from 78.04 to 76.97 for 37°C), and the imaginary part of the complex relative permittivity increased (from 11.49 to 14.07 for 37°C) with the increase of operation frequency from 4 GHz to 5 GHz.

3.4. Probe-Tip-Glucose Interaction. To visualize the electromagnetic field distribution during measurement, we simulated the electromagnetic field interaction between the probe-tip and glucose solution by using CST Microwave Studio software. The results are presented in Figure 5. From the simulated electromagnetic energy distribution, it is seen that as the glucose concentration increased from Di water, to 200 mg/ml, the relative permittivity of glucose solution was increased, and the electric energy density was increased from 9 mJ/m^3 to 19.5 mJ/m^3 at maximum. The impedance of probe-tip/sample system becomes less mismatched with impedance of the dielectric resonator, thus the amplitude of the reflection coefficient S_{11} was decreased. At the same time the magnetic energy density was still almost the same (not shown here). Note that the electric energy density exceeds the magnetic energy density by about 3 times at the same position.

4. Conclusions

We demonstrated the measurement of the glucose concentration using a microwave biosensor technique. The microwave reflection coefficient S_{11} was sensitive to the concentration of glucose in the solution and had a linear relation in the all concentration range. The measured SNR was about 37 dB, and the minimum detectible glucose concentration was about 1 mg/ml. These results show the sensitivity and the usefulness of this method for glucose sensing. This microwave biosensor has been particularly successful for the real-time monitoring of the concentration of glucose in aqueous solutions and mixtures. Practical development of this system will require significant advances in miniaturization and development of microwave sensing platforms with high specificity and long storage life, and integration with microfluidic devices and application-specific sampling systems.

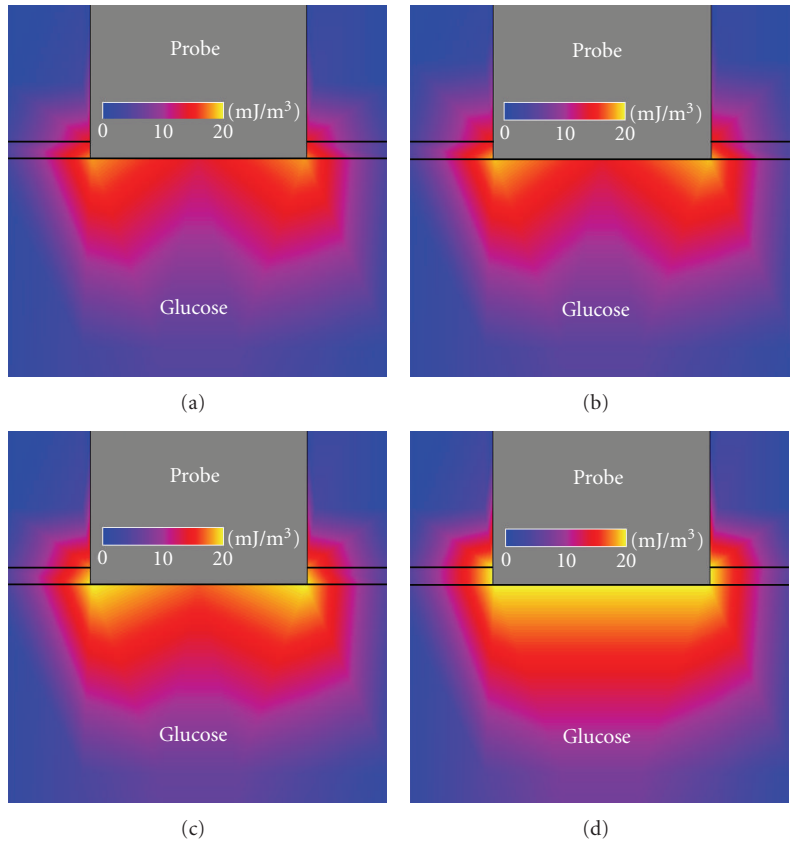

Figure 5: The simulated images for the electric energy densities of the electromagnetic interaction between the probe-tip and (a) DI water and glucose solution with the glucose concentration of (b) 10 mg/ml, (c) 100 mg/ml, and (d) 200 mg/ml. The glucose solution temperature was 37°C, and the operation frequency was 4.6 GHz.

Acknowledgments

This work was supported by Sogang University Special Research Grant (2010), Seoul Research and Business Development program (10816), Korea Research Foundation Grant (KRF-2008-615-C00001), and National Research Foundation of Korea Grant 2009-0093822 and 2010-0028297.

References

[1] J. Wang, "Glucose biosensors: 40 years of advances and challenges," *Electroanalysis*, vol. 13, no. 12, pp. 983–988, 2001.

[2] S. Zhang, G. Wright, and Y. Yang, "Materials and techniques for electrochemical biosensor design and construction," *Biosensors and Bioelectronics*, vol. 15, no. 5-6, pp. 273–282, 2000.

[3] A. Heller, "Implanted electrochemical glucose sensors for the management of diabetes," *Annual Review of Biomedical Engineering*, vol. 1, pp. 153–175, 1999.

[4] F. G. Tseng, K. H. Lin, H. T. Hsu, and C. C. Chieng, "A surface-tension-driven fluidic network for precise enzyme batch-dispensing and glucose detection," *Sensors and Actuators A*, vol. 111, no. 1, pp. 107–117, 2004.

[5] J. M. McKee and B. P. Johnson, "Real-time chemical sensing of aqueous ethanol glucose mixtures," *IEEE Transactions on Instrumentation and Measurement*, vol. 49, no. 1, pp. 114–119, 2000.

[6] M. Pan, X. Guo, Q. Cai, G. Li, and Y. Chen, "A novel glucose sensor system with Au nanoparticles based on microdialysis and coenzymes for continuous glucose monitoring," *Sensors and Actuators A*, vol. 108, no. 1–3, pp. 258–262, 2003.

[7] A. Subramanian, P. I. Oden, S. J. Kennel et al., "Glucose biosensing using an enzyme-coated microcantilever," *Applied Physics Letters*, vol. 81, no. 2, pp. 385–387, 2002.

[8] A. Babajanyan, K. Lee, R. Khachatryan, and K. Nerkararyan, "Sensing of glucose concentration by using a surface plasmon polariton," *Journal of the Korean Physical Society*, vol. 52, no. 2, pp. 440–443, 2008.

[9] B. Choudhury, R. Shinar, and J. Shinar, "Glucose biosensors based on organic light-emitting devices structurally integrated with a luminescent sensing element," *Journal of Applied Physics*, vol. 96, no. 5, pp. 2949–2954, 2004.

[10] M. Abu-Teir, M. Golosovsky, D. Davidov, A. Frenkel, and H. Goldberger, "Near-field scanning microwave probe based on a dielectric resonator," *Review of Scientific Instruments*, vol. 72, no. 4, pp. 2073–2079, 2001.

[11] B. Friedman, M. A. Gaspar, S. Kalachikov et al., "Sensitive, label-free DNA diagnostics based on near-field microwave imaging," *Journal of the American Chemical Society*, vol. 127, no. 27, pp. 9666–9667, 2005.

[12] D. E. Steinhauer, C. P. Vlahacos, S. K. Dutta, B. J. Feenstra, F. C. Wellstood, and S. M. Anlage, "Quantitative imaging of sheet resistance with a scanning near-field microwave microscope," *Applied Physics Letters*, vol. 72, no. 7, pp. 861–863, 1998.

[13] A. F. Lann, M. Golosovsky, D. Davidov, and A. Frenkel, "Combined millimeter-wave near-field microscope and capacitance distance control for the quantitative mapping of sheet resistance of conducting layers," *Applied Physics Letters*, vol. 73, no. 19, pp. 2832–2834, 1998.

[14] M. Tabib-Azar, "Evanescent microwaves: a novel super-resolution noncontact nondestructive imaging technique for biological applications," *IEEE Transactions on Instrumentation and Measurement*, vol. 48, no. 6, pp. 1111–1116, 1999.

[15] S. Kim, H. Yoo, K. Lee, B. Friedman, M. A. Gaspar, and R. Levicky, "Distance control for a near-field scanning microwave microscope in liquid using a quartz tuning fork," *Applied Physics Letters*, vol. 86, no. 15, Article ID 153506, pp. 1–3, 2005.

[16] A. Babajanyan, J. Kim, S. Kim, K. Lee, and B. Friedman, "Sodium chloride sensing by using a near-field microwave microprobe," *Applied Physics Letters*, vol. 89, no. 18, Article ID 183504, pp. 1–3, 2006.

[17] J. Kim, A. Babajanyan, A. Hovsepyan, K. Lee, and B. Friedman, "Microwave dielectric resonator biosensor for aqueous glucose solution," *Review of Scientific Instruments*, vol. 79, no. 8, Article ID 086107, pp. 1–3, 2008.

[18] K. Lee, A. Babajanyan, C. Kim, S. Kim, and B. Friedman, "Glucose aqueous solution sensing by a near-field microwave microprobe," *Sensors and Actuators A*, vol. 148, no. 1, pp. 28–32, 2008.

[19] S. Kim, J. Kim, A. Babajanyan, K. Lee, and B. Friedman, "Noncontact characterization of glucose by a waveguide microwave probe," *Current Applied Physics*, vol. 9, no. 4, pp. 856–860, 2009.

[20] J. Kim, M. S. Kim, K. Lee, J. Lee, D. Cha, and B. Friedman, "Development of a near-field scanning microwave microscope using a tunable resonance cavity for high resolution," *Measurement Science and Technology*, vol. 14, no. 1, pp. 7–12, 2003.

[21] D. Pozar, *Microwave Engineering*, Anderson-Wesley, New York, NY, USA, 2nd edition, 1990.

[22] E. Silva, M. Lanucara, and R. Marcon, "The effective surface resistance of superconductor/dielectric/metal structures," *Superconductor Science and Technology*, vol. 9, no. 11, pp. 934–941, 1996.

[23] D. Lide, *Handbook of Chemistry and Physics*, CRC Press, Boca Raton, Fla, USA, 85th edition, 2004.